DENTAL MATERIALS 27 (2011) 651–663

available at www.sciencedirect.com

ScienceDirect

journal homepage: www.intl.elsevierhealth.com/journals/dema

The effect of preparation order on the crystal structure of yttria-stabilized tetragonal zirconia polycrystal and the shear bond strength of dental resin cements

Ji-eun Moon[a], *Sung-hun Kim*[a,*], *Jai-bong Lee*[a], *Seung-ryong Ha*[b], *Yu-sung Choi*[c]

[a] *Department of Prosthodontics and Dental Research Institute, School of Dentistry, Seoul National University, 275-1, Yeongeon-dong, Jongno-gu, Seoul, Republic of Korea*

[b] *Department of Dentistry, School of Medicine, Ajou University, Suwon, Republic of Korea*

[c] *Department of Prosthodontics, College of Dentistry, Dankook University, Cheonan, Republic of Korea*

ARTICLE INFO

Article history:
Received 9 June 2010
Received in revised form
11 March 2011
Accepted 28 March 2011

Keywords:
Zirconia
Y-TZP ceramic
Shear strength
Resin cement

ABSTRACT

Objectives. The purpose of this study was to evaluate the effect of preparation order on the crystal structure of yttria-stabilized tetragonal zirconia polycrystal (Y-TZP) and the shear bond strength of dental resin cements.

Methods. One-hundred fifty pre-sintered Y-TZP cylinders (Ø 9 mm × 13.5 mm) were prepared and divided into three groups (control group, SBS group and SAS group). Specimens in control group were not treated. Specimens in SBS group were sandblasted and then densely sintered, and specimens in SAS group were sintered in advance, and then sandblasted. The specimens were analyzed by X-ray diffractometry, confocal laser scanning microscopy and Energy dispersive X-ray spectroscopy before and after sandblasting. All specimens were embedded in polytetrafluoroethylene (PTFE) molds using PMMA and each group was divided into five subgroups. The mixed resin cements (Clearfil SA luting cement, Zirconite, Superbond C&B, Rely-X Unicem, and Multilink) were placed onto the Y-TZP surfaces using PTFE molds with Ø 3 mm × 3 mm, followed by storage in distilled water at 37 °C for 24 h, and thermocycling (5000 cycles at 5 °C and 55 °C with a 30 s dwelling time). All specimens were tested for the shear bond strengths with a universal testing machine, and fractured surfaces were evaluated by SEM. Statistical analysis was performed using one-way ANOVA and Scheffé comparison with $\alpha = .05$.

Results. Sandblasting of the zirconia significantly increased shear bond strength of resin cements, but the preparation order had no significant influence on the shear bond strength in both test groups. In SEM observation, the natures of the surface faceting of the zirconia grains were totally different between SBS and SAS groups. SBS group exhibited less monoclinic structures than SAS group.

Significance. Sandblasting of pre-sintered Y-TZP and then sintering may induce favorable proportion of tetragonal structures. This might have positive effect on the clinical performance of zirconia restorations.

* *Corresponding author*. Tel.: +82 220722664; fax: +82 220723860.
E-mail address: ksh1250@snu.ac.kr (S.-h. Kim).

0109-5641/$ – see front matter © 2011 Academy of Dental Materials. Published by Elsevier Ltd. All rights reserved.
doi:10.1016/j.dental.2011.03.005

1. Introduction

Fixed partial denture materials are changing from porcelain fused to metal to all-ceramic systems due to their biocompatibility and esthetics [1]. The changes have been encouraged by the advent of zirconia with high fracture toughness [2–6]. Pure zirconia exists as a monoclinic (*m*) crystal structure at room temperature and transforms to tetragonal (*t*) structure at 1173 °C and cubic structure at 2370 °C. When zirconia is cooled down, its volume increases with the cubic or tetragonal to monoclinic transformation. This induces very large stresses within the material, and causes the zirconia to crack [1]. For dental applications, zirconia can be stabilized by the addition of 3 mol% yttrium oxide. As a results, yttria-stabilized tetragonal zirconia polycrystalline (Y-TZP) is metastable in its tetragonal crystalline at room temperature [7–9]. However, when the high stresses are applied to Y-TZP, the tetragonal phase is converted to monoclinic with 4–5% volume increase [9–12].

Sintered zirconia surface should be treated for the micromechanical retention of dental resin cements. Unlike glass ceramics, zirconia is not prone to hydrofluoric acid etching for surface treatment due to the polycrystalline and glass-free structures [13–16]. Thus, air-particle abrasion (sandblasting) has been suggested to roughen the zirconia surface [17]. However, due to the metastability of tetragonal zirconia, the surface treatment is responsible to trigger the transformation from tetragonal to monoclinic structure. This causes the strength reduction and the enhanced fracture tendency in zirconia because of the missing transformation capacity during critical loading. This is related to the amount of transformation, and may also damage the long-term lifespan of zirconia ceramics [18,19].

In general, the surface treatment for cementation is carried out after sintering of the zirconia. This may induce increased monoclinic phase of the zirconia. In order to reduce the monoclinic phase, an additional heat treatment should be done. Hence, it could be suggested that sandblasting of the pre-sintered zirconia in advance and then sintering procedure might generate less amount of monoclinic structures than sandblasting after sintering procedure. The purpose of this *in vitro* study was to evaluate the effect of preparation order on the crystal structure of zirconia and on the shear bond strengths of resin cements to zirconia ceramics. The two null hypotheses were that there is no difference (i) in the composition of crystal structures and (ii) in the shear bond strength of resin cements by preparation order on zirconia.

2. Materials and methods

2.1. Preparations of the specimens

The schematic test protocol used in this study is shown in Fig. 1. Specimens of 150 pre-sintered Y-TZP cylinders – which

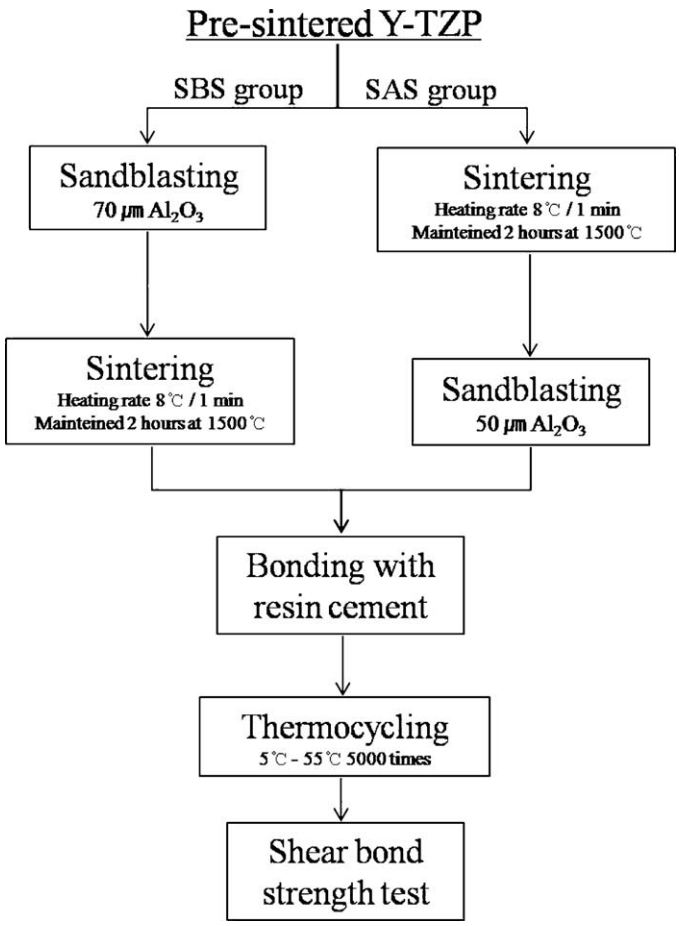

Fig. 1 – The schematic test protocol.

consisted of 88–96% ZrO_2, 4–6% Y_2O_3 and <1% Al_2O_3 – (Rainbow, Dentium, Seoul, Korea) of 9 mm diameter and 13.5 mm height were prepared and randomly divided into 3 groups. Control group (No Sandblasting; NS group) was not treated. One test group (Sandblasting Before Sintering; SBS group) was prepared with Al_2O_3 sandblasting in advance and then densely sintered at 1500 °C for 2 h. The other test group (Sandblasting After Sintering; SAS group) was densely sintered in advance at the same condition, and then sandblasted. Air-borne particle abrasion was done making circular movements at a stand-off distance of 10 mm with 3 bar pressure for 10 s. SAS group was sandblasted with 50 μm grain size, but SBS group was done with 70 μm grain size for the similar surface characteristics of the test groups, because pre-sintered Y-TZP tend to undergo their linear shrinkage of up to *circa* 20% during sintering [20,21]. All specimens were cleaned ultrasonically with distilled water in 5 min and rinsed for 1 min. The size of Y-TZP cylinder after densely sintering was 7 mm in diameter and 11 mm in height.

2.2. X-ray diffractometry

Before and after the sandblasting, the specimens were examined by X-ray diffractometry (XRD, Rigaku/JP-D/MAX-2500H, Berlin, Germany). XRD data was collected with 2θ diffractometer using the Cu-Kα radiation. Diffractogram was obtained from 20° to 70°, at a scan speed of 5°/min and a step size of 0.004° covering the location of the highest peaks of *t* and *m* ZrO_2 phases. The relative amount of transformed *m* structure (X_M) on the zirconia specimens' surfaces was calculated according to the method of Garvie and Nicholson [22].

2.3. Bonding procedure

Specimens of each group were randomly divided into 5 subgroups depending on each kind of resin cement applied ($N = 150$, $n = 10$). The abbreviations of the experimental groups, preparation order and the used resin luting cements are presented in Table 1.

Five commercial resin cements were used (Table 2). Three of them were dual-curing resin cements: Clearfil SA luting cement, Zirconite and Rely X Unicem and two were chemical-curing resin cements: Superbond C&B and Multilink.

All specimens were embedded in polytetrafluoroethylene (PTFE) molds (9 mm in inner diameter, 20 mm in outer diameter, and 11 mm in height) using polymethyl methacrylate (PMMA; Vertex-Dental, Dentimex, Zeist, Netherlands), constructing that one surface of the zirconia cylinder remained uncovered for adhering to the resin cement (Fig. 2a).

A PTFE ring with a hole (3 mm in inner diameter and 3 mm in height) was positioned on the uncovered zirconia surface. Base and catalyst of the resin cement were mixed and packed into the hole of the PTFE ring and then cured according to the manufacturers' recommendations. For specimens using Superbond C&B and Multilink, the corresponding primers (Porcelain Liner M and Metal/Zirconia Primer, respectively) were used. The primer was coated in a layer as thin as possible with a disposable brush. The PTFE ring was gently separated one side from the other 30 min after mixing the resin cement (Fig. 2b).

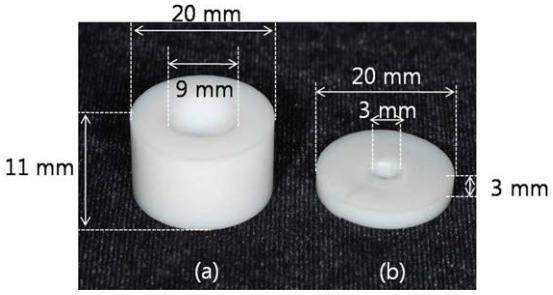

Fig. 2 – Polytetrafluoroethylene mold for embedding zirconia cylinder (a) and adhering resin cement (b).

All specimens were stored in distilled water for 24 h at 37 °C, followed by thermocycling (5000 cycles at 5 °C and 55 °C, with a 30 s dwelling time in each bath and 2 s of transferring time) [23].

2.4. Shear bond strength test

Specimens were mounted in the jig of a universal testing machine (Model 3345, Instron, Canton, MA, USA) and were loaded in shear at a constant crosshead speed of 0.5 mm/min until fracture. Maximum load to failure was recorded by the corresponding software in Newtons, and the shear bond strength was calculated in MPa.

2.5. Scanning electron microscopy (SEM), confocal laser scanning microscopy (CLSM) and energy dispersive X-ray spectroscopy (EDX)

Randomly selected specimens from all groups were gold-coated with a sputter coater (SC7620 Mini Sputter Coater, Polaron, Schwalbach, Germany) and then mounted on coded brass stubs and examined using the scanning electron microscope (VEGA II LSH, TESCAN, Brno, Czech Republic) at 180× and 5000× magnification and 20 kV accelerating voltage. Pre-sintered Y-TZP surfaces, sandblasted surfaces with 70 μm Al_2O_3, and surfaces after sintering were examined. In addition, sandblasted specimens with 50 μm Al_2O_3 after sintering were also examined, and were compared with former specimens.

Confocal laser scanning microscopy (CLSM, LSM 5 Pascal, Carl Zeiss Microscopy, Göttingen, Germany) was performed to confirm the similarity of the depths and widths of the scratches in last specimens of SBS group and SAS group. A 543 nm (1 mW) HeNe laser was used as a light source, and the specimens were observed at 200× magnification. The measuring area was 450 μm × 450 μm, and the height of the z-stack was 30 μm in 1 μm intervals.

The fractured interfacial surfaces of the specimens were also examined using SEM at 50× and 2000× magnification, and micro-analyzed by Energy dispersive X-ray spectroscopy (EDX, Horiba EX-250, Tokyo, Japan).

2.6. Statistical analysis

Statistical analyses were performed by using the statistical software (PASW Statistics 18.0 IBM Acquires SPSS Inc.,

Table 1 – Groups considering preparation order and the types of resin cements.

Group	Preparation order	Subgroup code	Resin cement
NS (Control)	No sandblasting	NSC	Clearfil SA luting cement
		NSZ	Zirconite
		NSR	Rely-X Unicem
		NSS	Superbond C&B
		NSM	Multilink
SBS	Sandblasting before sintering	SBSC	Clearfil SA luting cement
		SBSZ	Zirconite
		SBSR	Rely-X Unicem
		SBSS	Superbond C&B
		SBSM	Multilink
SAS	Sandblasting after sintering	SASC	Clearfil SA luting cement
		SASZ	Zirconite
		SASR	Rely-X Unicem
		SASS	Superbond C&B
		SASM	Multilink

Table 2 – List of brand names, curing types, main compositions, batch numbers and manufacturers of resin cements investigated.

Material	Type	Zirconia primer	Characteristics	Batch No.	Manufacturer
Clearfil SA luting cement	Dual-curing	×	Paste A: Bis-GMA, TEGDMA, MDP, DMA, Silanated barium glass filler, Silanated colloidal silica		
			Paste B: Bis-GMA, DMA, silanated barium glass filler, silanated colloidal silica, surface treated sodium fluoride	143BA	Kuraray Medical Co., Osaka, Japan
Zirconite	Dual-curing	×	Paste A: DMA, Methacrylated phosphoric acid esters, MPTMS, Fumed Silica	4146HQBARCZ	BJM Lab.,Or-Yehuda, Israel
			Paste B: Bis-GMA, TEGMA, 4-META		
Rely-X Unicem	Dual-curing	×	Powder: glass particles, initiators, silica, substituted pyrimidine, calcium hydroxide, peroxide composite and pigment	3922517	3 M ESPE, St Paul, MN, USA
			Liquid: methacrylate phosphoric acid ester, DMA, acetate, stabilizer and initiator.		
Superbond C&B	Self-curing	Porcelain Liner M	Powder: PMMA, Liquid: MMA, 4-META Catalyst: TBB	RE1	Sun Medical, Shiga, Japan
			+		
			Liquid A: MMA, 4-META	TG1	
			Liquid B: MMA, TMSPM	(Primer)	
Multilink	Self-curing	Metal/zirconia primer	Paste A: DMA, HEMA, fillers, BPO	NO7559	
			Paste B: DMA, HEMA, fillers, t-amine		IvoclarVivadent, Schaan, Lichtenstein
			+	M63563	
			DMA, phosphonic acid acrylate, initiator and stabilizer	(Primer)	

× = without zirconia primer; Bis-GMA = bis-phenol A diglycidylmethacrylate; TEGDMA = triethyleneglycoldimethacrylate; MDP = 10-methacryloyloxydecyl dihydrogen phosphate; DMA = dimethacrylate; MPTMS = 3-(methacryloyloxy)propyltrimethoxysilane; 4-META = 4-methacryloxyethyltrimellitic acid; PMMA = polymethyl methacrylate; MMA = methyl methacrylate; TBB = tri-N-butylborane; HEMA = 2-hydroxyethyl methacrylate; BPO = benzoyl peroxide; TMSPM = 3-(trimethoxysilyl)propyl methacrylate.

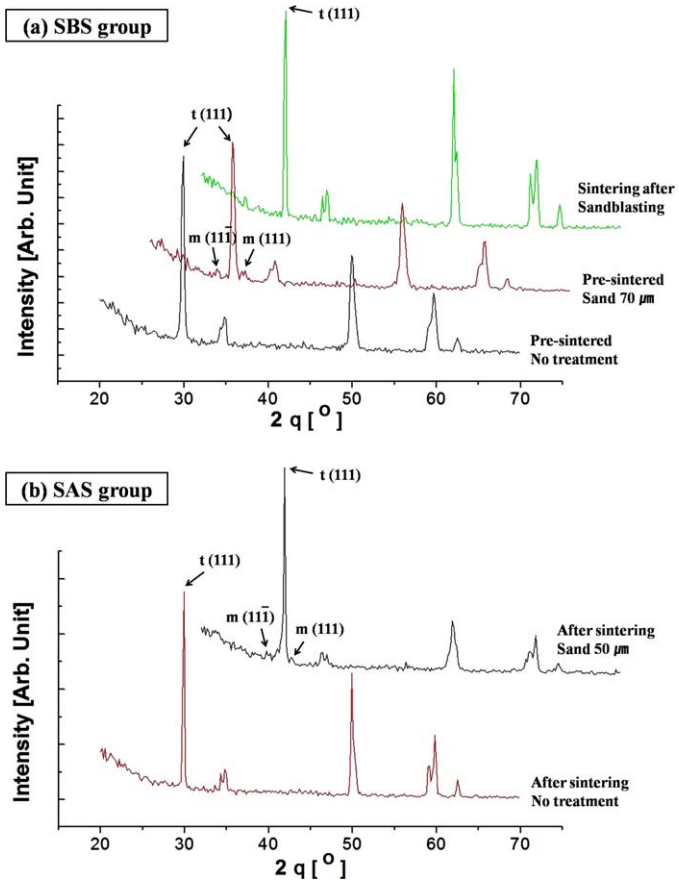

Fig. 3 – XRD patterns obtained from SBS and SAS groups. (a) In SBS, *m* phase peaks showed after sandblasting were disappeared with densely sintering procedure. (b) In SAS group, *m* phase peaks were appeared after sandblasting. Compared with the final graphs, *m* peaks presented higher intensity in SAS group.

Chicago, IL, USA). One-way analysis of variance and multiple comparison Scheffé post hoc tests were performed to verify the effect of preparation order, and two-sample *t*-tests were used to detect the differential effect of cements. The test was performed at a significance level of 0.05.

3. Results

3.1. *X-ray diffractometry*

According to the XRD patterns in SBS group, pre-sintered Y-TZP ceramics consisted of almost 100% tetragonal structures. After sandblasting with 70 μm Al_2O_3, detectable monoclinic peaks with marked preference of the M (1 1 $\bar{1}$) and M (1 1 1) appeared in the XRD pattern (Fig. 3a). Relative amount of the monoclinic phase on sandblasted pre-sintered specimen was 16.9%. After the sintering process, however, monoclinic peaks of M (1 1 $\bar{1}$) and M (1 1 1) were dramatically decreased to almost zero and were similar to the XRD pattern of no sandblasted pre-sintered Y-TZP ceramics. In SAS group, on the other hand, there were no monoclinic structures in sintered Y-TZP with no surface treatment (Fig. 3b), but after the sandblasting procedure, remarkable M (1 1 $\bar{1}$) and M (1 1 1) peak appeared. The monoclinic phase was 11.4%.

3.2. *Shear bond strength*

The mean values and the respective standard deviations of shear bond strength in all subgroups are listed in Table 3 and illustrated in Fig. 4. Superbond C&B plus Porcelain Liner M had the highest values, whereas Multilink plus Metal/Zirconia primer failed with the lowest values in all groups. In NS group, the second lowest value was obtained with Zirconite, but it showed the second highest value in SBS and SAS groups. The same sequence occurred in SBS and SAS groups, and there was no significant difference in shear bond strength between them.

3.3. *Scanning electron microscopy (SEM), confocal laser scanning microscopy (CLSM) and energy dispersive X-ray spectroscopy (EDX)*

Microscopic examination of the specimens revealed that erosive wears through chipping occurred during sandblasting which leveled the surface of pre-sintered and sintered zirconia materials (Fig. 5). The SEM image of pre-sintered zirconia specimen with no treatment shows microstructures of grained Y-TZP ceramics (Fig. 5a and b), but the sandblasted pre-sintered zirconia ceramic shows visible increased surface roughness in the topography (Fig. 5c and d). The surface

Table 3 – Mean values and standard deviations in parenthesis of shear bond strength (MPa) of resin cement investigated.

Code	Preparation order	Resin cement	Mean (SD)
NSC	No sandblasting	Clearfil SA luting cement[a]	3.43 (0.4)
NSZ		Zirconite[b]	1.22 (1.4)
NSR		Rely-X Unicem[a]	3.36 (0.8)
NSS		Superbond C&B	8.60 (3.9)
NSM		Multilink[b]	0.19 (0.2)
SBSC	Sandblasting before sintering*	Clearfil SA luting cement[c,d]	7.75 (3.3)
SBSZ		Zirconite[e]	12.81 (3.2)
SBSR		Rely-X Unicem[d,e]	9.04 (2.9)
SBSS		Superbond C&B	19.69 (3.7)
SBSM		Multilink[c]	4.10 (2.0)
SASC	Sandblasting after sintering*	Clearfil SA luting cement[f,g]	7.85 (2.3)
SASZ		Zirconite[h]	13.62 (3.3)
SASR		Rely-X Unicem[g]	8.63 (2.3)
SASS		Superbond C&B[h]	17.90 (4.8)
SASM		Multilink[f]	4.17 (1.5)

SD = standard deviation.
Same superscript letters denote subgroups which were not significantly different (Scheffé test: $p > 0.05$).

exhibited grain structures of Y-TZP ceramic after sintering and it has blunt and round edges (Fig. 5e and f). On the other hand, a densely sintered zirconia specimen before sandblasting (Fig. 5g and h) shows needle-like appearance after sandblasting (Fig. 5i and j).

The representative images measured by CLSM are shown in Fig. 6. Differences of specimen surfaces were verified from reconstructed 3-dimensional images.

The surface roughness (Sa) of the SBS group ($0.664 \pm 0.049\,\mu m$) and the SAS group ($0.654 \pm 0.072\,\mu m$) were similar, and there was no significant difference between them.

In SBS group, the graph of a middle base line of the specimen shows more irregular outlines (Fig. 6a). It seemed that the soft pre-sintered zirconia was affected by the sandblasting preparation more than the sintered zirconia. In SAS group, the graph outline shows uniform surface roughness (Fig. 6b).

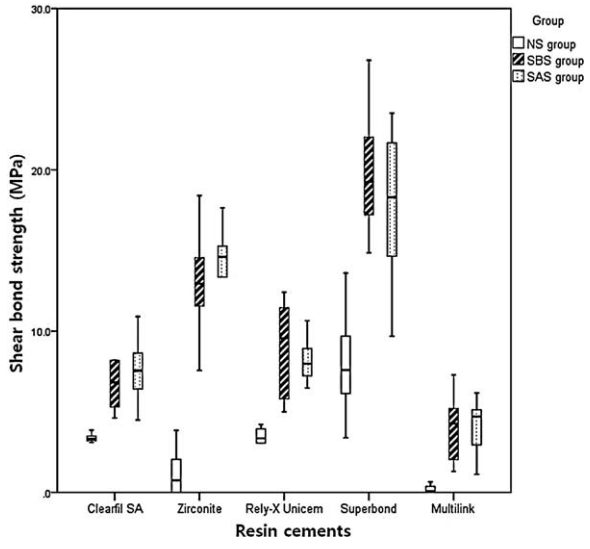

Fig. 4 – Box–plot diagram comprising the shear bond strengths (MPa) of 15 subgroups. ($n = 10$).

Figs. 7 and 8 show the representative SEM images and EDX spectra of the fractured interfaces in the specimens of Superbond C&B which exhibited the strongest shear bond strength to zirconia and Multilink which exhibited the weakest shear bond strength.

The EDX spectra reveal the composition of fractured surface sections of specimens, these spectra prove that high zirconium peaks and low oxide levels are shown in the zirconia section. On the other hand, EDX spectra obtained on the cement failure areas exhibit decreased zirconium peaks and obvious peaks of carbon due to the amount of remained resin cements, respectively.

As a control group, specimens in NSS group were examined under 50× magnification, and some residual cement were observed on the surface of specimens, especially around the marginal rim of the interfacial area (Fig. 7a). On the right side of EDX spectra of cement compared to the left side, the zirconia peak appeared shorter and carbon peak appeared weakly. On the other hand, specimens in NSM group were observed with almost no remnant cement, with zirconia surface being smooth and clean even under 2000× magnification (Fig. 8a).

It is difficult to distinguish the differences of zirconia crystal in the failure mode in the test group due to the strong bond strength to Superbond C&B (Fig. 7b and c). However, in subgroup SBSM, curls of zirconia grains and partially fractured resin cements are observed (Fig. 8a). Subgroup SASM shows the coarse and rough surface texture of zirconia grains with some cohesive failure of resin cements (Fig. 8b). In Fig. 8b and c, relatively small amount of cement is noted in fractured surfaces by cohesive failure mode compared to the Fig. 7b and c.

4. Discussion

Zirconia has acid-resistant or non-etchable characteristics [13–16]. Surface treatment of the zirconia such as sandblasting is recommended to improve bonding strength of

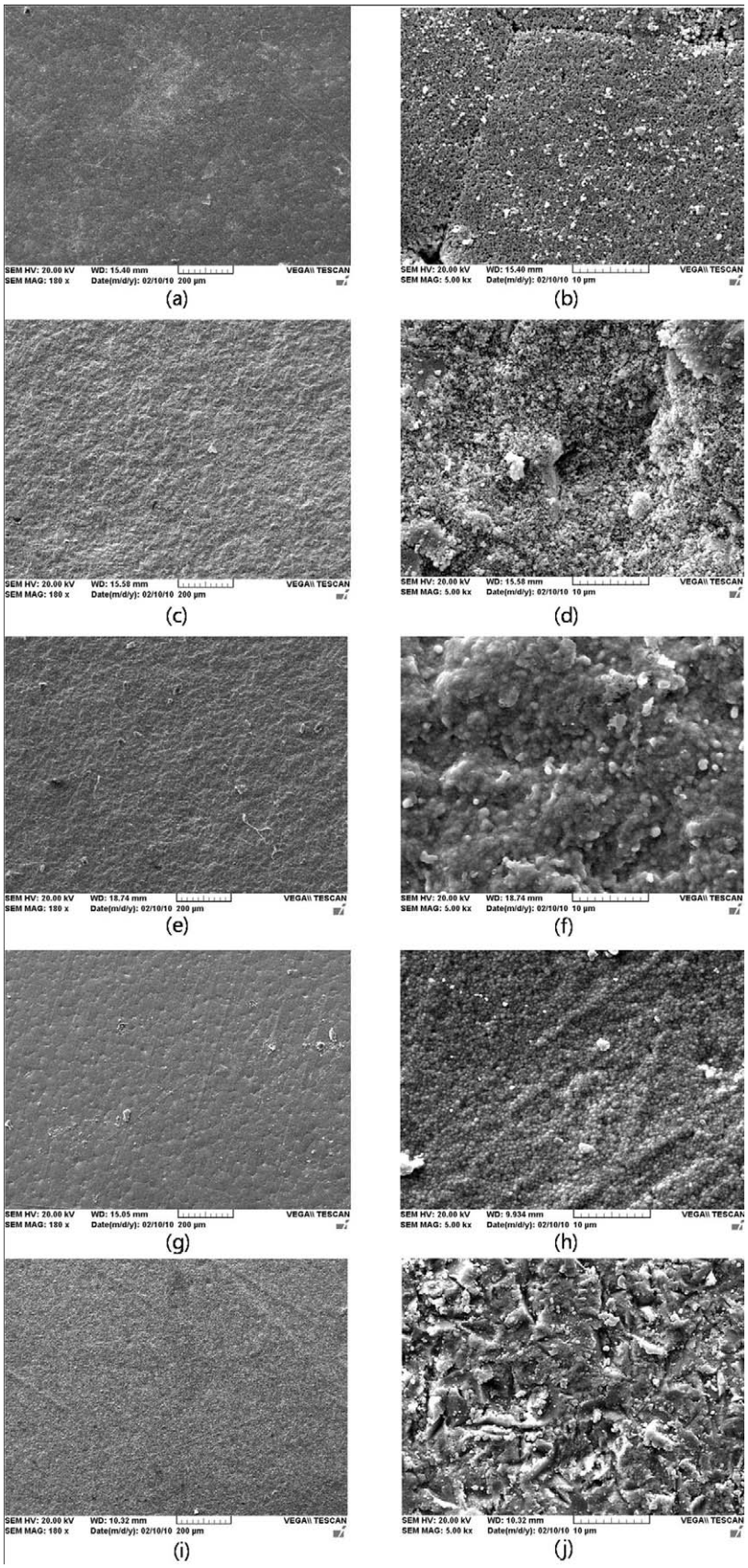

Fig. 5 – Scanning electron micrographs (the left sides magnification 180× and the right sides 5000×) of zirconia ceramic surfaces; (a, b) no treatment pre-sintered Y-TZP; (c, d) sandblasted pre-sintered Y-TZP; (e, f) sintered Y-TZP after early sandblasting; (g, h) no treatment sintered Y-TZP; (i, j) sandblasted Y-TZP after early sintering.

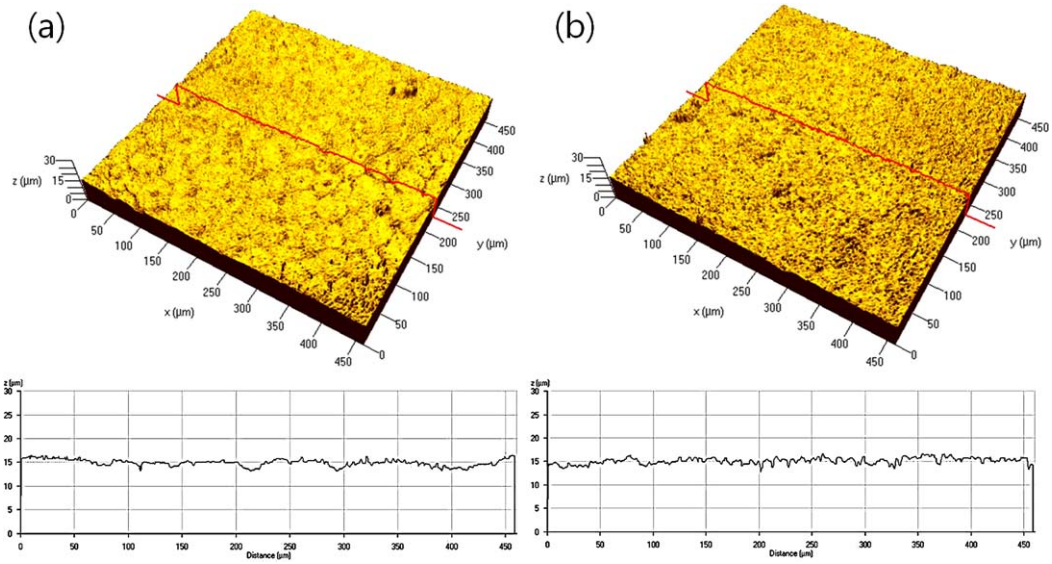

Fig. 6 – The representative CLSM images of the last step of each group specimens (a, b). (a) Sintered zirconia specimen undergone sandblasting in advance; (b) sandblasted zirconia specimen undergone sintering in advance.

resin cements [17,24–26]. However, it is considered that sandblasting generates stress on zirconia surfaces and accelerates $t \rightarrow m$ transformation [27,28]. In the SBS group, XRD pattern revealed lower monoclinic phase than in the SAS group. The relative monoclinic phase (X_M in %) of sandblasted pre-sintered Y-TZP specimens was 16.9%, but, the values dropped almost zero after sintering. This might be explained by that sandblasting procedure itself induced $t \rightarrow m$ transformation, but reverse transformation ($m \rightarrow t$) occurred during the sintering process [29]. The sandblasting process affected the zirconia crystal and surface structure on both groups, but the densely sintering process could reduce the proportion of monoclinic phase. Consequently, the final proportion of the monoclinic phase was almost zero in the SBS groups, but, 11.4% in the SAS groups. Therefore, the first null hypothesis that there is no difference in the composition of crystal structures by preparation order on zirconia could be rejected.

Control group displayed the lowest bonding strength. The highest bond strength value was recorded when Superbond C&B plus Porcelain Liner M were used on SBS group, but the value was not significantly different from that of SAS group. Like this, there was no significant difference of bond strength values in the same cements between two test groups. However, significant differences of bond strength values were shown among the resin cements. For instance, Superbond C&B with Porcelain Liner M (subgroup SBSS) showed the highest value (19.70 ± 3.7 MPa), while Multilink with Metal/Zirconia primer (subgroup SBSM) showed the lowest one (4.10 ± 2.0 MPa). Regardless of the significant differences in the shear bond strength among the resin cements, there were no significant differences of the bond strength between two test groups with different preparation order during procedure. In addition, all test groups with sandblasting exhibited a significant increase of bonding strength compared with the control group. Thus, the second null hypothesis that there is no difference in the shear bond strength of resin cements by preparation order on zirconia could be accepted.

The highest mean value of shear bond strength of resin cement was shown in Superbond C&B. This finding is in well agreement with other studies [5,30]. This might be explained by the viscosity of the resin cement [31]. The resin cement with low viscosity can flow easily into the microporosities of the sandblasted zirconia surface to have larger adhesion surfaces, but not when luted with high viscous resin cement, Multilink. In the figures of fracture photographs, the subgroups of Superbond C&B had higher rate of cohesive failure mode of resin cements than the subgroups of Multilink.

4-META and MDP in resin cements plays an important role in the bonding of resin cement to zirconia [32]. Previous studies have shown that 4-META and MDP act as coupling agents, due to the reaction between the hydroxyl groups in 4-META or the hydrogen groups in MDP and zirconia, similar to the reaction between silane coupling agents and silica-based ceramics [26,33]. Dérand and Dérand found that the filler-free resin cement containing 4-META/MMA-TBB exhibited the highest bond strength to Y-TZP [30]. This study showed similar results. The 4-META containing resin cements, Superbond C&B and Zirconite, exhibited the highest shear bond strength to zirconia surface. 4-META containing ceramic primer, Porcelain Liner M, might also influence the results. However, Zirconite in control group showed low value of bond strength, but in the sandblasted group it revealed the second highest bond strength. It seemed that the effect of 4-META in Zirconite was enhanced under the circumstances where micromechanical bonding is possible. Accordingly, when Zirconite

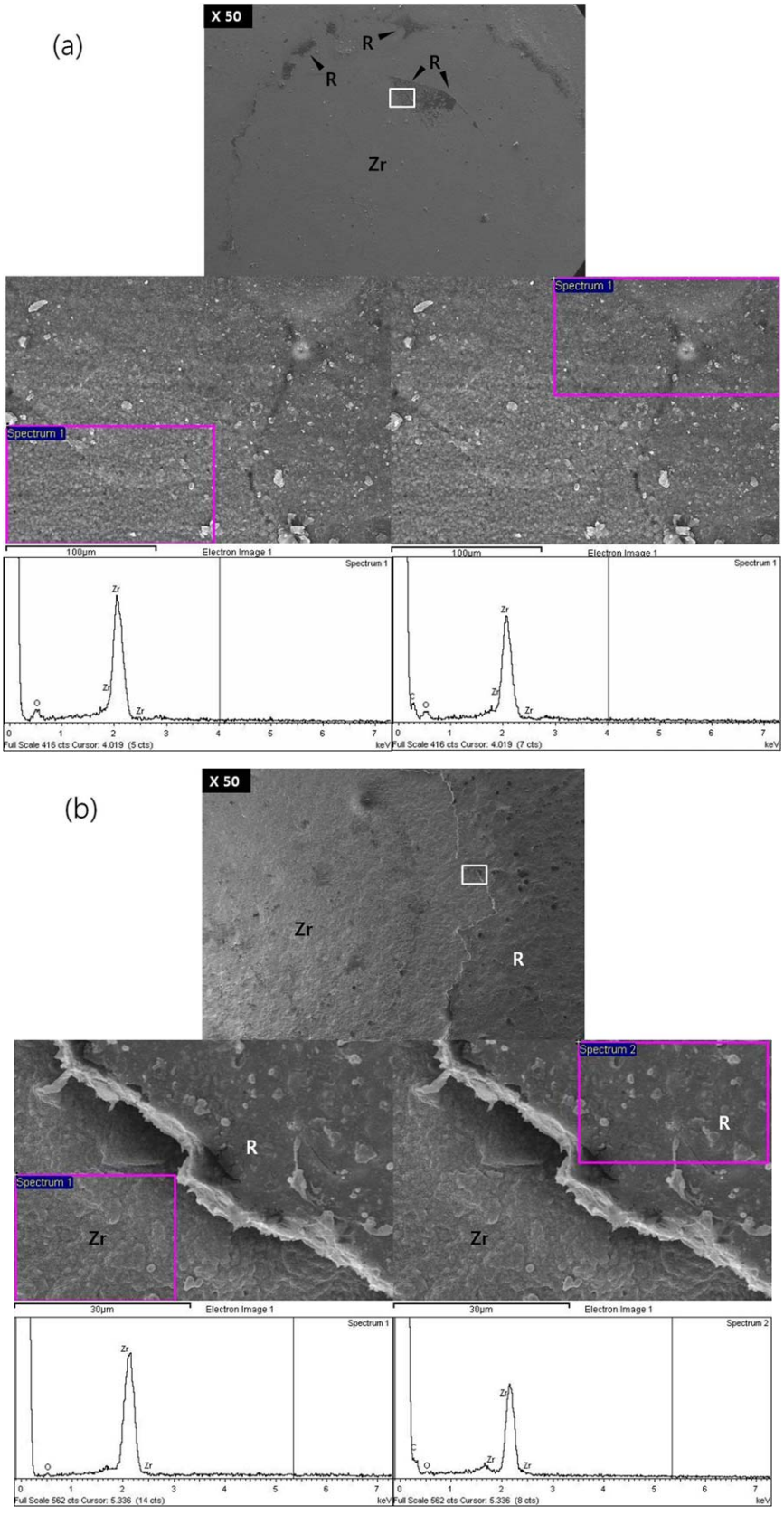

Fig. 7 – SEM photographs (at the top sides magnification 50× and the middle sides 2000×) and EDX spectra (at the bottom sides) of zirconia ceramic surfaces cemented with Superbond C&B (a–c): (a) specimen of group NSS; (b) specimen of group SBSS; (c) specimen of group SASS. R is represented resin cement, and Zr is represented zirconia.

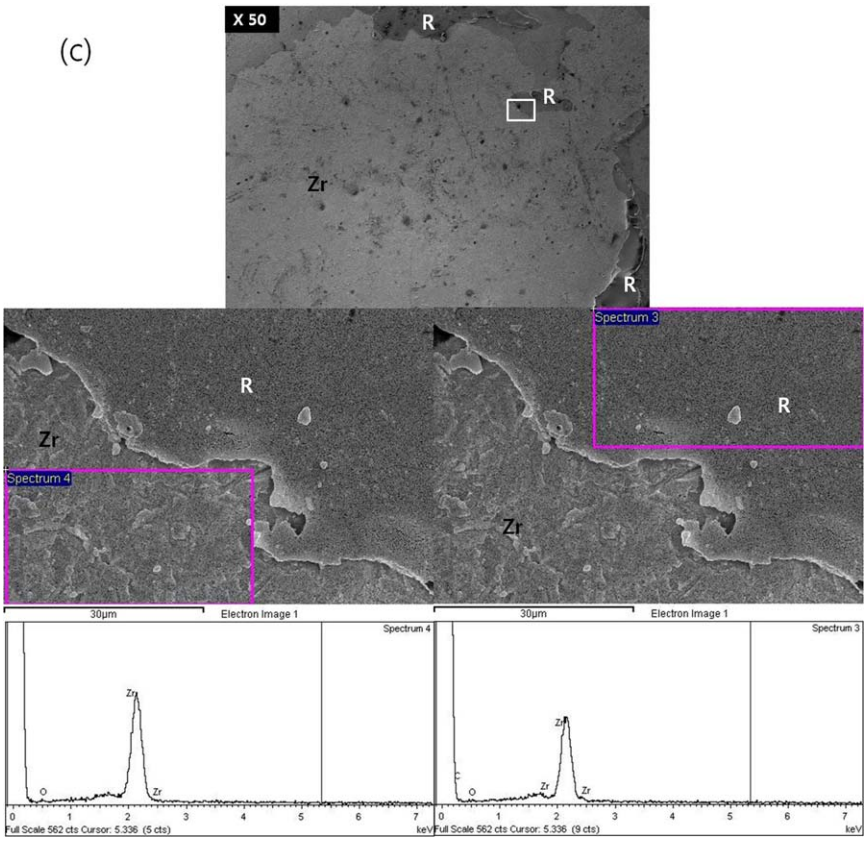

Fig. 7 – (*Continued*).

is used for the bonding with zirconia, sandblasting of the zirconia surface is necessary. However, the MDP-containing resin cement, Clearfil SA luting cement, showed relatively lower bonding strength than other cements. Further study of different MDP-containing resin cements should be carried out.

The micromechanical retention is very important for the bonding of resin cement. Both the penetration of the resin cement and *in situ* polymerization are responsible for the bonding of the resin cement to the ceramic restorations [34]. According to Tsuo et al., recommended air-borne particle size for sintered zirconia is 50 μm [20]. Another study concluded that air-borne particle abrasion with either smaller (50 μm) or larger (110 μm) particles is of beneficial for zirconia with a machined surface in terms of shear bond strength [21,35]. In this study, air-borne particle size of 50 μm was used in the SAS group and size of 70 μm was selected in the SBS group in order to obtain the similar surface roughness between the two test groups. This was confirmed by no significant differences in the surface roughness values (Sa) between them shown in Fig. 6. Interestingly, the SEM and 3D images showed that the natures of the surface feature of the zirconia grains were quite different between the SBS group and the SAS group (Figs. 5 and 6). Overall observation of the SBS group revealed that the specimens have blunt and melted-round surfaces. Whereas, the SAS group showed that the specimens had coarse and needle-like rough surfaces.

Within the limitations of this study, sandblasting of pre-sintered zirconia before sintering has several advantages. Firstly, the preparation order can produce surface roughness of zirconia ceramic with round depressions and projections. On the other hand, sandblasting of pre-sintered zirconia after sintering can produce sharp pointed dents and projections with needle-like edges which might cause the initiation of crack propagation in the zirconia and resin cement or increase their fracture potential. Secondly, the increased contents of the tetragonal structures after sintering can be achieved. This may improve the mechanical properties of zirconia ceramics. Thirdly, total fabrication time of zirconia restoration can be reduced because heat treatment to reduce monoclinic phase which was produced during sandblasting of the sintered zirconia can be omitted. However, there are possibilities of impairing the margin of zirconia coping and embedding of aluminum oxide particles into the zirconia ceramic during sandblasting of pre-sintered zirconia. In addition, this is technique sensitive, and demands precautions. Therefore, the further research must be carried out about standoff distance of sandblasting, shooting pressure, time taken and cleansing procedure for establishing the exact protocol. The clinical trials must be also carried out to prove the long-term effect of the preparation protocol.

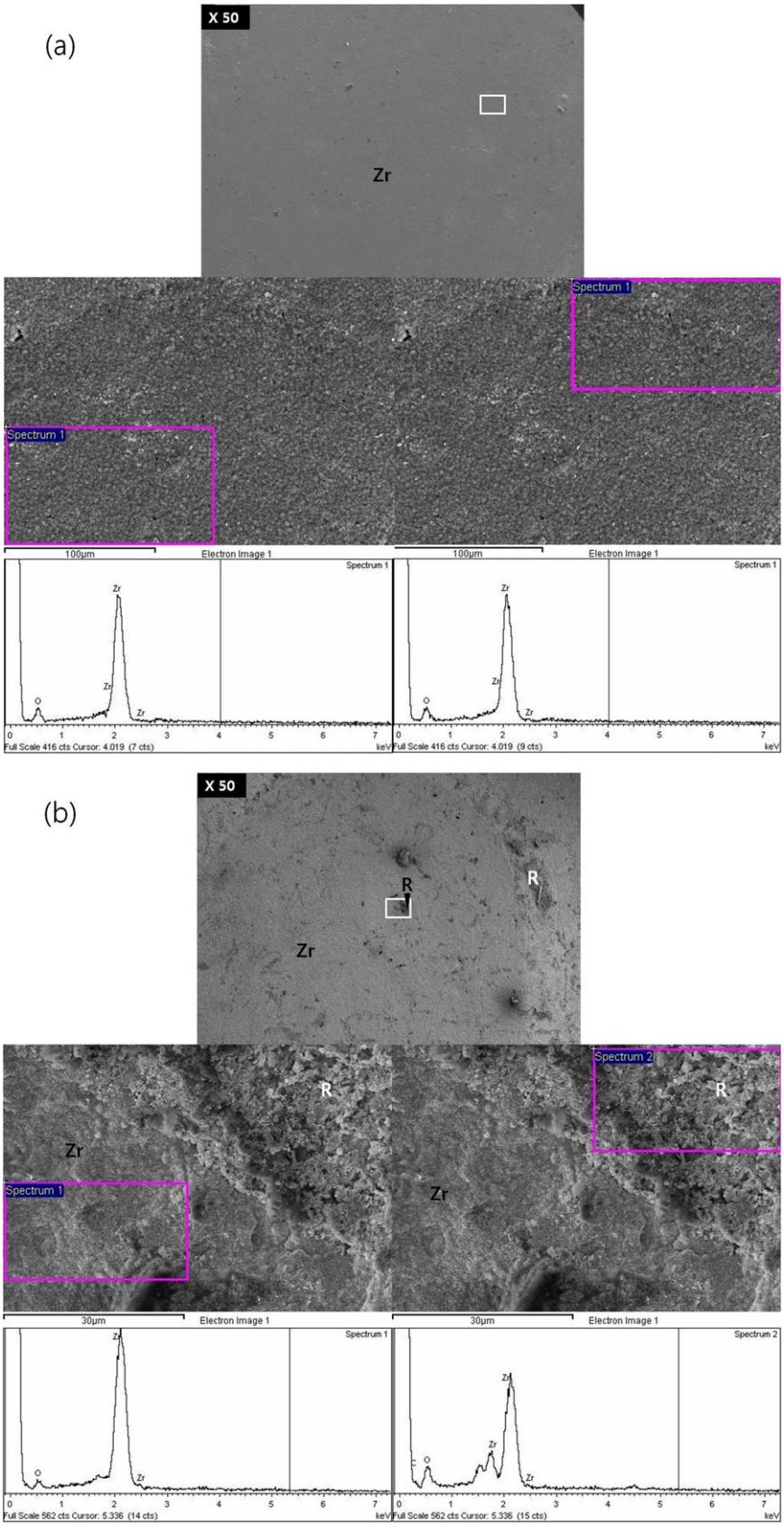

Fig. 8 – SEM photographs (at the topsidesmagnification 50× and the middle sides 2000×) and EDX spectra (at the bottom sides) of zirconia ceramic surfaces cemented with Multilink (a–c): (a) specimen of group NSM; (b) specimen of group SBSM; (c) specimen of group SASM. R is represented resin cement, and Zr is represented zirconia.

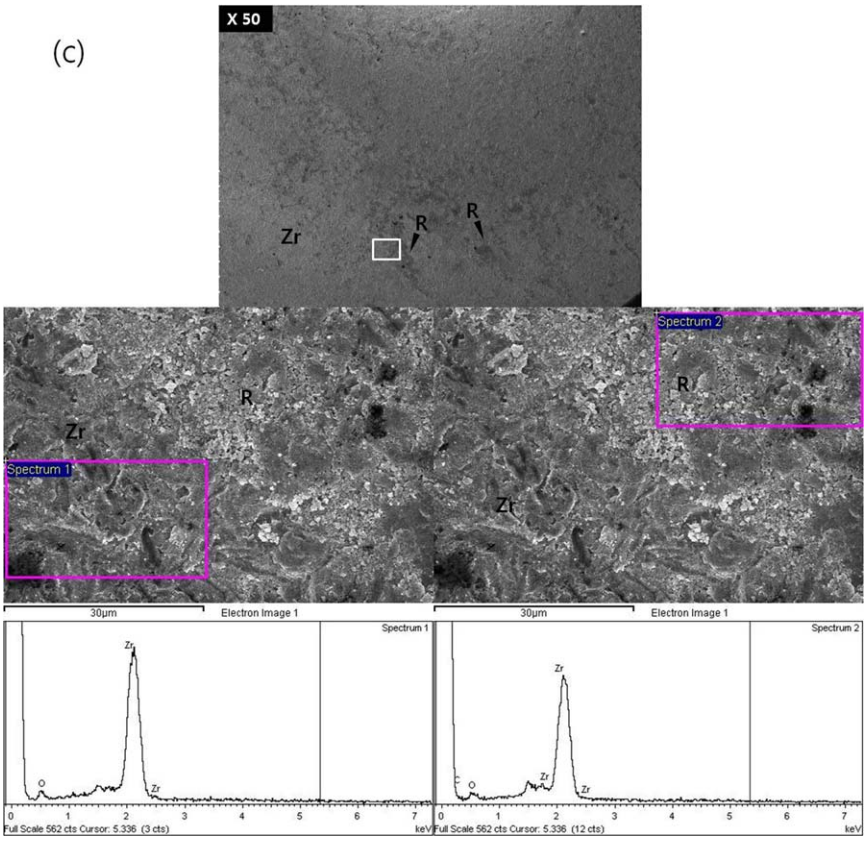

Fig. 8 – (*Continued*).

Acknowledgments

This study was supported by the research grant No. 03-2009-0017 from the Seoul National University Dental Hospital Research Fund.

The Y-TZP ceramic materials (Rainbow, Dentium, Seoul, Korea) used in this study were generously supplied by their manufacturers.

We are indebted to Dr. Byung-ho Yoon, Soon-hyo Park and Kwang-il Park of Genoss for technical XRD, scanning electron microscopy supports, and their advices.

REFERENCES

[1] Tholey MJ, Swain MV, Thiel N. SEM observations of porcelain Y-TZP interface. Dent Mater 2009;25:857–62.
[2] Fischer H, Weber M, Marx R. Lifetime prediction of all-ceramic bridges by computational methods. J Dent Res 2003;82:238–42.
[3] Luthardt RG, Holzhüter M, Sandkuhl O, Herold V, Schnapp JD, Kuhlisch E, et al. Reliability and properties of ground Y-TZP-zirconia ceramics. J Dent Res 2002;81:487–91.
[4] Suttor D, Bunke K, Hoescheler S, Hauptmann H, Hertlein G. LAVA – the system for all-ceramic ZrO_2 crown and bridge frameworks. Int J Comput Dent 2001;4:195–206.
[5] Ernst CP, Cohnen U, Stender E, Willershausen B. In vitro retentive strength of zirconium oxide ceramic crowns using different luting agents. J Prosthet Dent 2005;93:551–8.
[6] Giordano RA. Dental ceramic restorative systems. Compend Contin Educ Dent 1996; 17:779-82, 784-6 passim, 794.
[7] Richerson DW. Modern ceramic engineering: properties, processing, and use in design. New York: Marcel Dekker; 1992. pp. 756–762.
[8] Kelly JR, Denry I. Stabilized zirconia as a structural ceramic: An overview. Dent Mater 2008;24:289–98.
[9] Christel P, Meunier A, Heller M, Torre JP, Peille CN. Mechanical properties and short-term in vivo evaluation of yttrium-oxide–partially-stabilized zirconia. J Biomed Mater Res 1989;23:45–61.
[10] Lawson S. Environmental degradation of zirconia ceramics. J Eur Ceram Soc 1995;15:485–502.
[11] Zhang Y, Lawn BR, Rekow ED, Thompson VP. Effect of sandblasting on the long-term performance of dental ceramics. J Biomed Mater Res 2004;71B:381–6.
[12] Wolfart M, Lehmann F, Wolfart S, Kern M. Durability of the resin bond strength to zirconia ceramic after using different surface conditioning methods. Dent Mater 2007;23:45–50.
[13] Amaral R, Ozcan M, Bottino MA, Valandro LF. Microtensile bond strength of a resin cement to glass infiltrated zirconia-reinforced ceramic: the effect of surface conditioning. Dent Mater 2006;22:283–90.
[14] Atsu SS, Kilicarslan MA, Kucukesmen HC, Aka PS. Effect of zirconium-oxide ceramic surface treatments on the bond strength to adhesive resin. J Prosthet Dent 2006;95:430–6.
[15] Bottino MA, Valandro LF, Scotti R, Buso L. Effect of surface treatments on the resin bond to zirconium-based ceramic. Int J Prosthodont 2005;18:60–5.
[16] Blatz MB, Sadan A, Kern M. Resin-ceramic bonding: a review of the literature. J Prosthet Dent 2003;89:268–74.
[17] Qeblawi DM, Muñoz CA, Brewer JD, Monaco Jr EA. The effect of zirconia surface treatment on flexural strength and shear

bond strength to a resin cement. J Prosthet Dent 2010;103:210–20.
[18] Schubert H, Frey F. Stability of Y-TZP during hydrothermal treatment: neutron experiments and stability considerations. J Eur Ceram Soc 2005;25:1597–602.
[19] Shimizu K, Oka M, Kumar P, Kotoura Y, Yamamuro T, Makinouchi K, et al. Time-dependent changes in the mechanical properties of zirconia ceramic. J Biomed Mater Res 1993;27:729–34.
[20] Tsuo Y, Yoshida K, Atsuta M. Effect of alumina-blasting and adhesive primers on bonding between resin luting agent and zirconia ceramics. Dent Mater J 2006;25:669–74.
[21] Heydecke G, Butz F, Binder JR, Strub JR. Material characteristics of a novel shrinkage-free $ZrSiO_4$ ceramic for the fabrication of posterior crowns. Dent Mater 2007;23:785–91.
[22] Garvie RC, Nicholson PS. Phase analysis in zirconia systems. J Am Ceram Soc 1972;55:303–5.
[23] Ernst CP, Canbek K, Euler T, Willershausen B. In vivo validation of the historical in vitro thermocycling temperature range for dental materials testing. Clin Oral Invest 2004;8:130–8.
[24] Özcan M, Vallittu PK. Effect of surface conditioning methods on the bond strength of luting cement to ceramics. Dent Mater 2003;19:725–31.
[25] Valandro LF, Özcan M, Bottino MC, Bottino MA, Scotti R, Bona AD. Bond strength of a resin cement to high-alumina and zirconia-reinforced ceramics: the effect of surface conditioning. J Adhes Dent 2006;8:175–81.
[26] Yoshida K, Tsuo Y, Atsuta M. Bonding of dual-cured resin cement to zirconia ceramic using phosphate acid ester monomer and zirconate coupler. J Biomed Mater Res B Appl Biomater 2006;77:28–33.
[27] Peterson IM, Pajares A, Lawn BR, Thompson VP, Rekow ED. Mechanical characterization of dental ceramics by herzian contacts. J Dent Res 1998;77:589–602.
[28] Kosmac T, Oblak C, Jevnikar P, Funduk N, Marion L. The effect of surface grinding and sandblasting on flexural strength and reliability of Y-TZP zirconia ceramic. Dent Mater 1999;15:426–33.
[29] Michael VS, Richard H, Hannink J. Metastability of the martensitic transformation in a 12 mol% Ceria-Zirconia Alloy: II, grinding studies. J Am Ceram Soc 2005;72:1358–64.
[30] Dérand P, Dérand T. Bond strength of luting cements to zirconium oxide ceramics. Int J Prosthodont 2000;13:131–5.
[31] Hahn P, Attin T, Gröfke M, Hellwig E. Influence of resin cement viscosity on microleakage of ceramic inlays. Dent Mater 2001;17:191–6.
[32] Ueno T, Kumagai T, Hirota K. The characteristic of metal primer 'GC METAL PRIMER II'. J Dent Res 1997;76(Special Issue 312):Abstract No. 2385.
[33] Atsuta M, Nagata K, Turner DT. Strong composites of dimethacrylates with 4-methacryloxyethyl trimellitic anhydride. J Biomed Mater Res 1983;17:679–90.
[34] Borges GA, Sophr AM, de Goes MF, Sobrinho LC, Chan DC. Effect of etching and airborne particle abrasion on the microstructure of different dental ceramics. J Prosthet Dent 2003;89:479–88.
[35] Phark JH, Duarte Jr S, Blatz M, Sadan A. An in vitro evaluation of the long-term resin bond to a new densely sintered high-purity zirconium-oxide ceramic surface. J Prosthet Dent 2009;101:29–38.